

РАДІОЕЛЕКТРОНІКА ТА ТЕЛЕКОМУНІКАЦІЇ

RADIO ELECTRONICS AND TELECOMMUNICATIONS

UDC 621.396.67

POWER SUPPLY OF RING ANTENNA USING DIRECTIONAL COUPLERS

Ilitskiy L. Ya. – Dr. Sc., Honored Worker of Science and Technology of Ukraine, National Aviation University, Kyiv, Ukraine.

Shcherbyna O. A. – Dr. Sc., Professor of the Department of Electronics, Robotics and Technology of Monitoring and Internet of Things, National Aviation University, Kyiv, Ukraine.

Zaliskyi M. Yu. – Dr. Sc., Professor of the Department of Telecommunication and Radio Electronic Systems, National Aviation University, Kyiv, Ukraine.

Mykhalchuk I. I. – PhD, Assistant of the Department of Cyber Security and Information Protection, Taras Shevchenko National University, Kyiv, Ukraine.

Kozhokhina O. V. – PhD, Associate Professor of the Department of Avionics, National Aviation University, Kyiv, Ukraine.

ABSTRACT

Context. The circular polarization of radio waves is used in various electronic systems. This includes, for example, space communications stations, some radio relay communication systems, radar stations, data transmission systems and others. The characteristics of radio wave propagation are studied by using electromagnetic waves separated by circular orthogonal polarization in radiomonitoring and radiocontrol systems. Compared to other antenna types, circularly polarized antennas, such as rings, have superior design simplicity and excellent electrodynamic properties.

Objective. The objective of this study is to analyse the characteristics and application of directional microstrip couplers for supplying power to ring antennas.

Method. To better the performance of microstrip ring antennas, the reasons for their limited operating frequency range are analysed. These causes include the frequency-dependent parameters of the coupler, errors in calculating the directional coupler circuit, and radiation from asymmetric strip lines. To understand how supply lines, affect antenna characteristics, correlations between radiation fields determined in both its coordinate system and that of the primary axis are taken into account.

Results. An analysis of the dependence graphs of the main characteristics of ring microstrip antennas with intricate power supply circuits for directional couplers and comparison with similar characteristics for simple circuits revealed that the shape of the radiation pattern in the higher radiation hemisphere became symmetrical about the axis, especially when symmetrically supplying the ring with branch-line couplers. The frequency band has also widened, at which there was an acceptable degree of deviation in the ellipticity coefficient from unity.

Conclusions. The simulation results of microstrip ring antennas with power lines connected to directional couplers of different types showed that supplying the ring antenna with electricity via the directional coupler ensures circular polarization for the emitted electromagnetic waves. Additionally, the range of operating frequencies where there is only a small discrepancy in ellipticity coefficient remains at an acceptable level of -3 dB is quite broad. By utilizing directional branch-line couplers to power a ring antenna, it is possible to simultaneously emit both right and left circularly polarized waves with the same antenna.

KEYWORDS: microstrip ring antenna, directional microstrip coupler, supply lines, ellipticity coefficient, main coordinate system, individual coordinate system.

ABBREVIATIONS

AA is an antenna array;
RHCP is right-handed circular polarization;
VSWR is the voltage standing wave ratio.

NOMENCLATURE

$C = 30kl_{eff}$ is the constant value for the emitter;
 $F(\theta, \varphi)$ is the directivity characteristic of linear conductors in the main coordinate system;

$F_{\theta}(\theta)$ and $F_{\theta}(\varphi)$ are directivity characteristics of the ring antenna in different planes;

$F(\alpha, \beta)$ is the directivity characteristic of linear conductors in the individual coordinate system;

I_0 is current amplitude of the ring antenna at $\varphi = 0$.

$\dot{I}_{s,l}$ is the complex amplitude of the current flowing around the emitter;

$J_0(\sin\theta)$, $J_1(\sin\theta)$, $J_2(\sin\theta)$ are Bessel functions of the 0th, 1st and 2nd order;

$k = 2\pi\lambda$ is the wave number;
 K_e is the ellipticity coefficient;
 \vec{l}'_0 and \vec{m}'_0 are unit vectors of the rectangular coordinate system $l'0, m'$;
 l_{eff} is the effective length of the linear emitter;
 m is the ratio of the meridional component of the field intensity to the azimuthal value;
 q is the radiation efficiency factor of the strip line transmission;
 α, β, ρ are coordinates of the individual spherical coordinate system;
 $\alpha_0, \beta_0, \rho_0$ are unit vectors of the individual spherical coordinate system;
 θ, φ, r are coordinates of the main spherical coordinate system;
 θ_0, φ_0, r_0 are unit vectors of the main spherical coordinate system;
 λ is the length of the electromagnetic wave.
 $\xi = c/v_f$ is the ratio of the speed of electromagnetic wave propagation in free space to the speed of wave in the strip line.
 ρ is the distance from the phase center O_1 to the observation point M .
 ψ is the phase shift of the emitter current $I_{s,l}$ relative to the current phase of the ring antenna in the cross-section of the conductor with the coordinate $\varphi = 0$;

INTRODUCTION

The circular polarization of radio waves is used in various electronic systems. This includes, for example, space communications stations, some radio relay communication systems, radar stations, data transmission systems and others. The characteristics of radio wave propagation are studied by using electromagnetic waves separated by circular orthogonal polarization in radiomonitoring and radiocontrol systems. Compared to other antenna types, circularly polarized antennas, such as rings, have superior design simplicity and excellent electrodynamic properties.

The ring antenna stands out for its uncomplicated construction and excellent electrical features when it comes to sending and receiving circularly or rotational polarized electromagnetic waves. It is composed of a conductor twisted in a loop, usually about the same length as the wavelength of an electric current. An antenna of this type can separate the wave that hits it into two components with circular polarization [1, 2], a phenomenon which is crucial to understanding the polarization properties of the radiation field. However, when it comes to actually constructing a ring antenna, it can be difficult to develop and construct the appropriate supplying device. One potential way of constructing the necessary circuitry for supplying the ring antenna is through using directional couplers.

Considering the current trend toward the prevalent utilization of PCB technology to make ring radiators and their supplying systems, this study examines the

principles of constructing microstrip ring antennas on couplers with electromagnetic coupling and branch-line couplers.

The object of this study is the process of separating an electromagnetic wave into two components with different directions of circular polarization orientations.

The subject of this study is the method for constructing directional couplers for the power circuit of a microstrip ring antenna.

The objective of this study is to analyse the characteristics and application of directional microstrip couplers for supplying power to ring antennas.

1 REVIEW OF THE LITERATURE

Scientific papers provide information on a wide variety of ring antenna designs. The article [3] considers a basic slotted microstrip antenna with a capacitive as an element to generate radiation with circular polarization. Articles [4, 5] discuss a slotted ring antenna array (AA), which can switch between the S- and C-bands or between the S, C, and X bands, respectively. The 2x2 AA diagonal supplying process is used when operating in C-band mode. This technique offers the maximum level of decoupling for both vertical and horizontal polarizations. The article [6] presents a dual-band annular slot AA for both L and C bands. The aperture of the L-band slot antenna can be transformed into a 2x2 AA for the C-band using pin diodes. The design presented in the study [7] is a broadband single-layer ring antenna with a low level of cross-polarization. The ring elements can be combined into an AA to address different issues, such as measuring electromagnetic field parameters. In the paper [8] a double annular-ring microstrip antenna, split into six sectors, is proposed to achieve multiband operation with high gain and impedance bandwidth. The gaps on the driven and parasitic patches excite resonant frequencies that are located in the Ku-, K-, and Ka-bands thus making the antenna capable of these multiband applications. In the article [9] the design process of an annular ring microstrip antenna using graphene material for dualband applications is proposed. The microstrip antenna is modified using graphene-based annular ring microstrip layers for patch and ground plane with FR-4 epoxy substrate in between. The design process applied the short-pin technique for the estimation of the return loss, which leads to the analysis of the resonant frequency and the dual-band directions. Meanwhile, paper [10] outlines the principles of constructing the AA using ring elements.

It is widely recognized that a directional coupler, when connected to an electromagnetic wave transmission line, extracts a specific amount of electromagnetic energy from the transmission line and separates the incident and reflected waves in a predetermined power ratio. This property of the directional coupler can be applied to feed the ring antenna or receive electromagnetic waves while separating them in a circular orthogonal polarization basis.

Studies [1, 2] indicate that during the receiving mode, the electrical processes in the conductor of the ring

antenna can be regarded as two waves that move towards each other. These waves run around the antenna in a circular orthogonal polarization basis, with one wave rotating in a clockwise direction and the other in a counter clockwise direction. Consequently, the ring antenna can be considered as a transmission line in which the incident and reflected waves propagate during the receiving mode. To select the wave with the appropriate right or left direction around the ring antenna, it is recommended to use a directional coupler.

2 PROBLEM STATEMENT

Fig. 1 depicts a directional coupler with electromagnetic coupling where the conductor segment of the ring represents the primary line of the device. The primary line (numbered 1–2 in Fig. 1) is connected to the secondary line (numbered 3–4). Since the coupler formed by the stripline segments of the transmission lines is backward, a voltage is generated in shoulder 3 that is proportional to the current wave running counter clockwise around the ring. To ensure proper operation of the directional coupler, port 4 must be loaded with an impedance equal to the wave impedance of strip 3–4.

The operational principle of the circuit suggests that it is advisable to utilize the directional coupler with electromagnetic coupling only in the mode of receiving radio waves. This is due to the device's low efficiency, as a portion of the energy supplied to lines 3–4 is lost at the matched impedance of port 4.

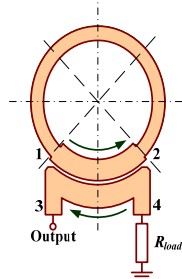


Figure 1 – The ring antenna with supplying by a directional coupler with electromagnetic coupling

In contrast, the branch-line directional coupler is a more efficient option, as depicted in Fig. 2.

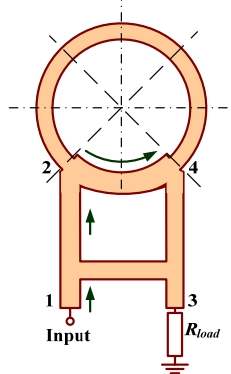


Figure 2 – The ring antenna with supplying by a branch-line directional coupler

Ports 1 and 3 of the branch-line directional coupler are electrically isolated, enabling the supply of current to both ports from two generators of identical frequency in the antenna transmission mode. This allows for the formation of a radiation field with any desired ellipticity coefficient. During the receiving mode, voltages are generated in ports 1 and 4, which are proportional to the intensity vectors of the electric fields rotating in the right and left directions. When the ring antenna is powered by a single generator connected to port 1 in the transmission mode, port 3 is loaded with a matched impedance. However, with the correct construction of the coupler, no energy enters or is absorbed into a load of port 4. Consequently, the efficiency of the device approaches unity.

The devices shown in Fig. 1 and Fig. 2 were studied using a specialized simulation program in the radiation mode of electromagnetic waves with right-handed circular polarization (RHCP). For the study, the operating frequency of $f = 1.2$ GHz ($\lambda = 0.25$ m) was selected, and the substrate for microstrip models was a dielectric with relative permittivity of $\epsilon_r = 4.4$, a dielectric loss tangent of $\text{tg}\delta = 0.002$, and a substrate thickness of $h = 1.6$ mm.

The results of the simulation are illustrated by the radiation patterns in two planes (Fig. 3), and the frequency dependence of the wave ellipticity coefficients, as shown in Fig. 4. In both cases, the voltage standing wave ratio (VSWR) within the operating frequency band did not exceed 1.5. Moreover, the directivity factor for the investigated right-handed circular polarization (RHCP) type was not less than 4 dBi.

Based on the results obtained from modelling ring antennas connected by directional couplers with an electromagnetic oscillation generator, the following conclusions can be drawn:

1. Supplying the ring with the directional coupler facilitates the study of electromagnetic waves on a circular orthogonal polarization basis. For the directional branch-line coupler to provide circular polarization with the directional branch-line coupler, it is necessary to design it with a power division factor of 3 dB.

2. The acceptable range operating frequency with a permissible deviation of the ellipticity coefficient from unity is significantly wide. This range can fulfill the requirements for the ellipticity of radiated waves in communication systems in certain cases.

3. Supplying a ring antenna with devices constructed using directional couplers allows for the creation of antennas with controlled polarization characteristics of the radiation field. This observation pertains to power devices constructed on branch-line directional couplers.

4. The simple power schemes, depicted in Fig. 1 and Fig. 2 tend to limit the operating frequency range of the ring antenna. This outcome is undesired, particularly when using these antennas for metrological purposes.

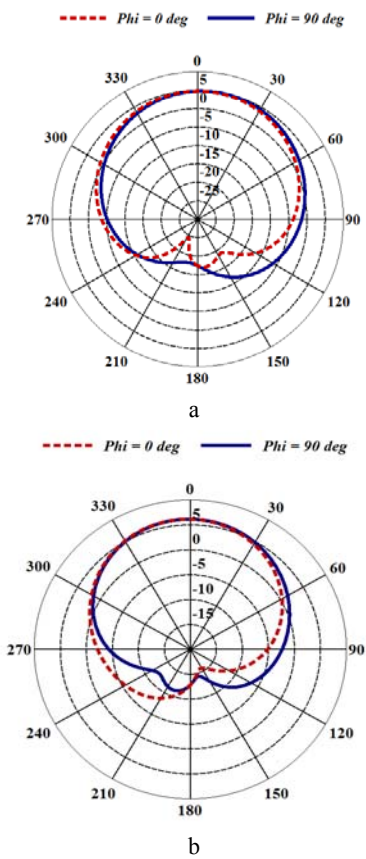


Figure 3 – Radiation patterns of ring antennas in two planes ($\varphi = 0$ and $\varphi = 90^\circ$): a – powered by a directional coupler with electromagnetic coupling; b – powered by a branch-line directional coupler

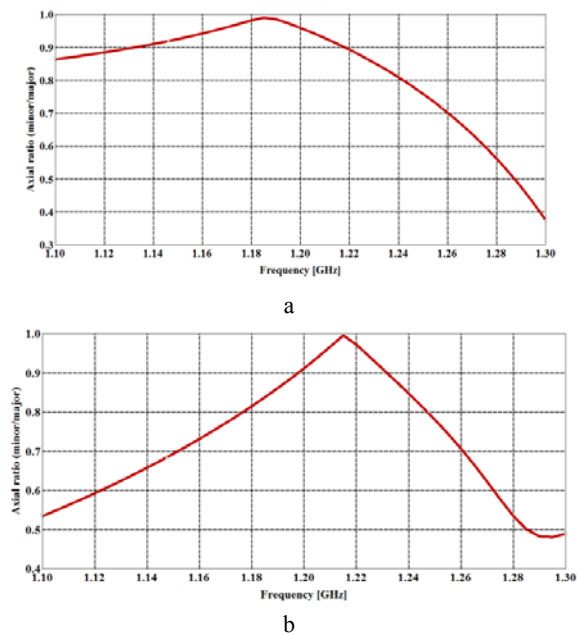


Figure 4 – Dependencies of the ellipticity coefficient of ring antennas on the operating frequency in the direction $\theta = 0$: a – powered by a directional coupler with electromagnetic coupling; b – powered by a branch-line directional coupler

To enhance power devices and improve their properties, it is essential to examine the primary factors that contribute to the narrowing of the operating frequency range of the antenna. The most significant factor that influences the frequency response of the ring with the power supply is the frequency dependence of the parameters of the directional coupler. It is therefore evident that it is necessary to use coupler designs that ensure the stability of the primary parameters within specific frequency ranges.

The second significant factor is the accuracy of the directional coupler circuit calculation. Since one of the directional coupler components is the ring segment, determining the wave impedance of this segment poses a challenge. The radiation of electromagnetic waves by an annular strip line complicates the calculation of wave impedance.

The third factor that affects the structure of the radiation field of the ring antenna is the radiation of asymmetric strip lines [11, 12], which are utilized in constructing the power supply devices for the ring. The radiation intensity of strip lines is usually negligible, so in most cases, this can be neglected. However, when designing measurement antennas with stringent requirements for metrological characteristics, it is necessary to consider possible deformations of the radiation field structure due to the superposition of the fields of the ring antenna and segments of strip lines.

3 MATERIALS AND METHODS

As is known [1], the radiation field of the ring antenna is analytically described in the spherical coordinate system r, θ, φ , the polar axis of which coincides with the circle axis and the Oz axis of the rectangular coordinate system x, y, z . The antenna itself is located in the xOy plane of the rectangular coordinate system. Both coordinate systems are considered primary. Without considering the specific power supply system of the ring antenna, it is assumed that the radiation of the transmission line segment, which is part of the power supply system, is similar to the radiation of a short linear dipole. When the output impedance of the directional coupler is fully matched with the wave impedance of the ring, the current flowing through the elements of the power supply is determined uniquely through the current in the conductors of the ring.

To utilize the dipole radiation field formula, it is necessary to assign a coordinate system (both spherical and rectangular) to the power supply element, in which electromagnetic processes in the dipole are analysed. Consequently, the polar axis of this coordinate system, designated as O_1l , must coincide with the axis of the supply line. Since the axis of the segment of the power circuit element, as well as the element itself, is in the xOy plane of the main coordinate system, it is advisable to place another coordinate axis in the same plane, for example, the O_1m axis, in the coordinate system associated with the radiating element, and the third axis O_1n parallel axis Oz ($\theta = 0$). The new coordinate systems are denoted

as follows: rectangular l, m, n and spherical ρ, α, β , where 0_1l is the polar axis ($\alpha = 0$). In spherical coordinate system, α is the meridional angle, β is the azimuth angle. Such coordinate systems are considered to be the emitter's own coordinate systems. The mutual position of the coordinate systems is shown in Fig. 5.

The origin of the main coordinate system (point 0) coincides with the phase center of the ring antenna, and point 0_1 is the phase center of the interference emitter, that is, a segment of the strip line of the power device. In the general case, the axis of the interference emitter will not be parallel to the axes $0x$ and $0y$, therefore, Fig. 5 shows the axes $0_1l'$ and $0_1m'$, which are parallel to the axes of the main coordinate system and are shifted from the corresponding axes of the own coordinate system by an angle Δ .

Fig. 5 also shows the observation point M , the position of which in the main coordinate system is defined as $M(r, \theta, \varphi)$, and in the emitter's own system as $M(\rho, \alpha, \beta)$.

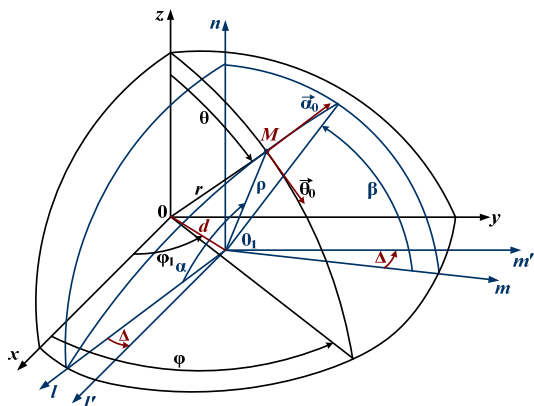


Figure 5 – The mutual position of the main and individual coordinate systems

The intensity of the interference electric field at point M in its coordinate system is written as

$$\dot{E}_{int} = \vec{\alpha}_0 \frac{qCl_{s,l}}{\rho} F(\alpha, \beta) e^{-ik\rho}. \quad (1)$$

To evaluate the impact of such field on the ring antenna radiation, it is necessary to determine the vector $\vec{\alpha}_0$ from expression (1), and the angles α and β using the quantities $\vec{\theta}_0, \vec{\varphi}_0$ and r, θ, φ . To accomplish this, the polar axis in its individual coordinate system must be altered, with the 0_1n axis designated as the polar axis. The meridional angle will be measured from the 0_1n axis, while the azimuthal angle τ – will be measured from the 0_1l axis (Fig. 5 and Fig. 6).

In the own coordinate system ρ, α, β , the unit vector $\vec{\rho}_0$ is determined by the coordinates of the rectangular coordinate system m, n, l , which can be expressed as:

$$\vec{\rho}_0 = \vec{m}_0 \sin \alpha \cos \beta + \vec{n}_0 \sin \alpha \sin \beta + \vec{l}_0 \cos \alpha. \quad (2)$$

In the ρ, σ, τ system, the value of the unit vector can be determined using the following expression:

$$\vec{\rho}_0 = \vec{l}_0 \sin \sigma \cos \tau + \vec{m}_0 \sin \sigma \sin \tau + \vec{n}_0 \cos \sigma. \quad (3)$$

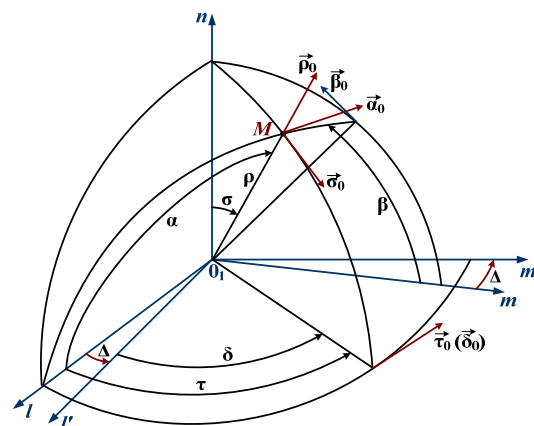


Figure 6 – The mutual position of two coordinate systems m, n, l and m', n', l' with angular shift Δ

As the right parts of expressions (2) and (3) represent the same value, it is possible to find the relation between the angles α, β and σ, τ . So

$$\left. \begin{aligned} \sin \alpha \cos \beta &= \sin \sigma \sin \tau; \\ \sin \alpha \sin \beta &= \cos \sigma; \\ \cos \alpha &= \sin \sigma \cos \tau. \end{aligned} \right\} \quad (4)$$

From the equations system (4):

$$\left. \begin{aligned} \cos \alpha &= \sin \sigma \cos \tau; \\ \sin \alpha &= \sqrt{1 - \cos^2 \tau \sin^2 \sigma}; \\ \cos \beta &= \frac{\sin \sigma \sin \tau}{\sqrt{1 - \cos^2 \tau \sin^2 \sigma}}; \\ \sin \beta &= \frac{\cos \sigma}{\sqrt{1 - \cos^2 \tau \sin^2 \sigma}}. \end{aligned} \right\} \quad (5)$$

Transforming to the rectangular coordinate system m, n, l , the expression for the unit vector $\vec{\alpha}_0$ in the own coordinate system can be written as follows:

$$\vec{\alpha}_0 = \vec{m}_0 \cos \alpha \cos \beta + \vec{n}_0 \cos \alpha \sin \beta - \vec{l}_0 \sin \alpha. \quad (6)$$

Equations (5) and (6) determine the values of the vector $\vec{\alpha}_0$ in the new coordinate system, where the polar axis aligns with the 0_1n axis:

$$\vec{\alpha}_0 = \left(1 - \cos^2 \tau \sin^2 \sigma\right)^{\frac{1}{2}} \begin{bmatrix} \vec{m}_0 \cos \tau \sin^2 \sigma \sin \tau + \\ + \vec{n}_0 \cos \sigma \cos \tau \sin \sigma - \\ - \vec{l}_0 (1 - \cos^2 \tau \sin^2 \sigma) \end{bmatrix}. \quad (7)$$

After shifting the coordinate system by an angle Δ (Fig. 6), the new coordinate system can be obtained with axes $0_1l'$ and $0_1m'$ parallel to the axes $0x$ and $0y$ of the main system, by using the following equations:

$$\left. \begin{aligned} \vec{l}_0 &= \vec{l}'_0 \cos \Delta - \vec{m}'_0 \sin \Delta; \\ \vec{m}_0 &= \vec{l}'_0 \sin \Delta + \vec{m}'_0 \cos \Delta. \end{aligned} \right\} \quad (8)$$

Using relation (8), the dependence of the vector $\vec{\alpha}_0$ (7) on the unit vectors of the coordinate system $l'0_1m'$ can be found:

$$\begin{aligned} \vec{\alpha}_0 &= \vec{l}'_0 \frac{\sin^2 \sigma \cos(\delta + \Delta) \cos \delta - \cos \Delta}{\sqrt{1 - \cos^2(\delta + \Delta) \sin^2 \sigma}} + \\ &+ \vec{m}'_0 \frac{\sin^2 \sigma \cos(\delta + \Delta) \sin \delta + \sin \Delta}{\sqrt{1 - \cos^2(\delta + \Delta) \sin^2 \sigma}} + \\ &+ \vec{n}_0 \frac{\cos \sigma \sin \sigma \cos(\delta + \Delta)}{\sqrt{1 - \cos^2(\delta + \Delta) \sin^2 \sigma}}. \end{aligned} \quad (9)$$

The spherical coordinate system ρ, σ, δ is combined with the rectangular coordinate system (Fig. 6). To express the formula (9) in the spherical coordinate system, the formula (9) is substituted with the values of orts \vec{l}'_0, \vec{m}'_0 and \vec{n}_0 expressed in terms of the coordinates and orts of the system ρ, σ, δ :

$$\left. \begin{aligned} \vec{l}'_0 &= \vec{\rho}_0 \sin \sigma \cos \delta + \vec{\sigma}_0 \cos \sigma \cos \delta - \vec{\delta}_0 \sin \delta; \\ \vec{m}'_0 &= \vec{\rho}_0 \sin \sigma \sin \delta + \vec{\sigma}_0 \cos \sigma \sin \delta + \vec{\delta}_0 \cos \delta; \\ \vec{n}_0 &= \vec{\rho}_0 \cos \sigma - \vec{\sigma}_0 \sin \sigma. \end{aligned} \right\}$$

After substituting and rearranging the expressions, we obtain:

$$\begin{aligned} \vec{\alpha}_0 &= -\vec{\sigma}_0 \frac{\cos \sigma \cos(\delta + \Delta)}{\sqrt{1 - \cos^2(\delta + \Delta) \sin^2 \sigma}} + \\ &+ \vec{\delta}_0 \frac{\sin(\delta + \Delta)}{\sqrt{1 - \cos^2(\delta + \Delta) \sin^2 \sigma}}. \end{aligned} \quad (10)$$

So, the vector $\vec{\alpha}_0$ in the spherical coordinate system ρ, σ, δ has two mutually perpendicular components that are orthogonal to the vector $\vec{\rho}_0$. One component is in the meridional plane and the other is in the azimuth plane.

The impact of the interference field (1) on the field of the ring antenna can be estimated only by determining the relationship between the values ρ, σ, δ included in the formula (1) and the values r, θ, φ of the main coordinate

system. To establish this connection, it is necessary to refer to Fig. 5, where the position of the phase center of the interference source in the main coordinate system is denoted by x_1 and y_1 . The distance between the phase centers of the ring antenna and interference sources is defined as:

$$d = \sqrt{x_1^2 + y_1^2}.$$

The distance between the phase center of the ring antenna and the observation point M in the main rectangular coordinate system can be expressed as:

$$r = \sqrt{x^2 + y^2 + z^2}, \quad (11)$$

where x, y, z are the coordinates of point M .

The distance from the phase center of the interference source 0_1 to the observation point M can be calculated as follows:

$$\rho = \sqrt{(x - x_1)^2 + (y - y_1)^2 + z^2} \quad (12)$$

In the spherical coordinate system, the coordinates of the observation point M can be expressed as follows:

$$\left. \begin{aligned} x &= r \sin \theta \cos \varphi; \\ y &= r \sin \theta \sin \varphi. \end{aligned} \right\} \quad (13)$$

The position of the phase center of the interference source in the spherical coordinate system is as follows:

$$\left. \begin{aligned} x_1 &= d \cos \varphi_1; \\ y_1 &= d \sin \varphi_1. \end{aligned} \right\} \quad (14)$$

Using relations (11), (15) and (16), the right-hand side of equation (12) can be simplified to the following form:

$$\rho = \sqrt{r^2 + d^2 - 2dr \sin \theta \cos(\varphi - \varphi_1)}$$

or

$$\rho = r \sqrt{1 + \left(\frac{d}{r}\right)^2 - 2\frac{d}{r} \sin \theta \cos(\varphi - \varphi_1)}. \quad (15)$$

If the observation point is in the far field, then $d \ll r$ and the formula (15) can be written as follows:

$$\rho = r - d \sin \theta \cos(\varphi - \varphi_1) \quad (16)$$

In the case when the distance ρ is used in the calculation of quantities in which the slight difference between the distance ρ and the distance r can be neglected, it can be assumed that

$$\rho \approx r. \quad (17)$$

Therefore, the value ρ from formula (16) should be taken into account in the exponent in expression (1), and in other cases, the approximate value (17) is used.

To establish a relation between the meridional angles θ and σ can be found through the expression:

$$\sigma = \arccos(z/\rho). \quad (18)$$

Since the z -coordinate in the main coordinate system is equal to

$$z = r \cos \theta, \quad (19)$$

then expression (18), in which relations (15) and (19) are used, becomes a function of the meridional angle σ of the coordinate system ρ , σ , δ which depends on the parameters θ and φ of the main coordinate system:

$$\sigma = \arccos \left(\frac{\cos \theta}{\sqrt{1 + \left(\frac{d}{r}\right)^2 - 2 \frac{d}{r} \sin \theta \cos(\varphi - \varphi_1)}} \right)$$

or it can be written approximately that $\sigma \approx \theta$.

The azimuthal angle δ of the observation point M in the main coordinate system can be determined as shown in Fig. 7:

$$\delta = \arctg((y - y_1)/(x - x_1)). \quad (20)$$

As depicted in Fig. 7, the meridional planes passing through point M in both coordinate systems intersect at an angle Ω . Therefore, it can be written that:

$$\delta = \varphi - \Omega. \quad (21)$$

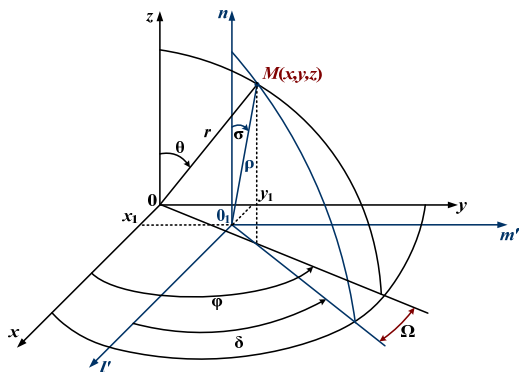


Figure 7 – The mutual position of two coordinate systems x, y, z and l', m', n

Since the angle φ can be determined through the coordinates of the observation point as $\varphi = \arctg(x/y)$, then the value of the angle Ω can be found as the difference between the angles φ and δ :

$$\Omega = \arctg(x/y) - \arctg((y - y_1)/(x - x_1)). \quad (22)$$

By using expressions (15) and (14), it is possible to represent expression (22) in terms of the observation point's coordinates in the basic spherical coordinate system as follows:

$$\Omega = \chi\pi + \arctg \frac{d \sin(\varphi_1 - \varphi)}{r \sin \theta - d \cos(\varphi_1 - \varphi)}, \quad (23)$$

where $\chi = 0$ if $A > -1$; $\chi = +1$ if $A < -1$ and $\text{tg} \varphi > 0$;
 $\chi = -1$ if $A < -1$ and $\text{tg} \varphi < 0$;
 $A = \text{tg} \varphi \frac{r \sin \theta \sin \varphi - d \sin \varphi_1}{r \sin \theta \cos \varphi - d \cos \varphi_1}$.

If the inequalities $y \gg y_1$ and $x \gg x_1$ are valid, it can be assumed that:

$$\delta \approx \varphi. \quad (24)$$

The spherical surfaces $r = \text{const}$ and $\rho = \text{const}$ intersect at point M as shown in Fig. 7. As a result, the tangent planes at point M are not parallel to each other. Only at significant distances from points O and O_1 , where condition (20) is satisfied, it can be assumed that the planes $\theta M \varphi$ and $\sigma M \delta$ coincide. In this case, the corresponding unit vectors of the polar coordinate system in the plane tangent to point M (Fig. 8) will be displaced from one another by an angle Ω .

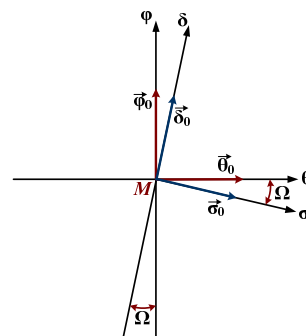


Figure 8 – The shift of unit vectors of the spherical coordinate system

In this regard, expression (10) in the coordinates θ and φ can be rewritten as follows:

$$\vec{\alpha}_0 = \vec{\theta}_0 A_\theta + \vec{\varphi}_0 A_\varphi, \quad (25)$$

where

$$A_\theta = \frac{\sin(\varphi + \Delta - \Omega) \sin \Omega}{\sqrt{1 - \cos^2(\varphi + \Delta - \Omega) \sin^2 \theta} - \frac{\cos \theta \cos(\varphi + \Delta - \Omega) \cos \Omega}{\sqrt{1 - \cos^2(\varphi + \Delta - \Omega) \sin^2 \theta}}};$$

$$A_\varphi = \frac{\sin(\varphi + \Delta - \Omega) \cos \Omega}{\sqrt{1 - \cos^2(\varphi + \Delta - \Omega) \sin^2 \theta} - \frac{\cos \theta \cos(\varphi + \Delta - \Omega) \sin \Omega}{\sqrt{1 - \cos^2(\varphi + \Delta - \Omega) \sin^2 \theta}}}.$$

The directivity characteristic is another factor present in expression (1), and its content is dependent on the chosen coordinate system. To determine the directivity characteristic, the reasons for the radiation of the power

supply elements must be considered and specified. The traveling wave mode is established in the transmission line segments with the correct construction of the device. When asymmetric strip lines are used for energy transfer, surface waves arise, leading to the generation of a radiation field. The directivity characteristic of linear conductors with a traveling wave of current is known and can be expressed as follows for our case:

$$F(\alpha, \beta) = \cos \alpha \frac{\sin \left[\frac{kl}{2} (\xi - \cos \alpha) \right]}{\frac{kl}{2} (\xi - \cos \alpha)}. \quad (26)$$

Formula (26) needs to be modified in the general case to account for the screen effect. To transform this formula into the dependence of the noise field intensity on the coordinates of the main polar coordinate system, we can use expressions (5), (17), (20), (21), (23), or (24).

Since the strip lines are designed to minimize or eliminate radiation, the value of q in formula (1), which represents the radiation efficiency coefficient, is much less than unity. Therefore, the efficiency coefficient characterizes the losses in asymmetric strip lines due to the radiation of electromagnetic energy.

Considering all the obtained relationships between the coordinates of the individual and the main coordinate systems, the radiation field of the interference source can be expressed as follows:

$$\vec{E}_{int} = (\vec{\theta}_0 A_\theta + \vec{\varphi}_0 A_\varphi) q CI_{s,l} F(\theta, \varphi) e^{i\nu\varphi} e^{-ikr}.$$

For the ring antenna, the radiation field is defined as:

$$\vec{E}_{ring} = (\vec{\theta}_0 F_\theta(\theta) - i\vec{\varphi}_0 F_\varphi(\theta)) \frac{30\pi I_0}{r} e^{-ikr},$$

where $F_\theta(\theta) = 2ctg\theta J_1(\sin\theta)$;

$$F_\varphi(\theta) = J_0(\sin\theta) - J_2(\sin\theta).$$

In the meridional plane, the electric field intensity of both the antenna and the interference is equal:

$$\vec{E}_\theta = \vec{E}_{ring}^\theta + \vec{E}_{int}^\theta e^{-i\nu\varphi} = E_\theta e^{i\nu\varphi} e^{i\omega t}, \quad (27)$$

where $E_{ring}^\theta = \frac{30\pi I_0}{r} F_\theta(\theta)$; $E_{int}^\theta = q A_\theta CI_{s,l} F(\theta)$;

$$E_\theta = \sqrt{(E_{ring}^\theta)^2 + 2E_{ring}^\theta E_{int}^\theta \cos \psi + (E_{int}^\theta)^2};$$

$$\psi_\theta = \arccos \left(\frac{E_{ring}^\theta + E_{int}^\theta \cos \psi}{E_\theta} \right) = \arcsin \left(-\frac{E_{int}^\theta \sin \psi}{E_\theta} \right).$$

In the horizontal plane, the sum of the intensities is determined as follows:

$$\vec{E}_\varphi = \vec{E}_{ring}^\varphi e^{-i\frac{\pi}{2}} + \vec{E}_{int}^\varphi e^{-i\nu\varphi} = E_\theta e^{i\nu\varphi} e^{i\omega t}, \quad (28)$$

where $E_{ring}^\varphi = \frac{30\pi I_0}{r} F_\varphi(\theta)$; $E_{int}^\varphi = q A_\varphi CI_{s,l} F(\theta)$;

$$E_\varphi = \sqrt{(E_{ring}^\varphi)^2 + 2E_{ring}^\varphi E_{int}^\varphi \sin \psi + (E_{int}^\varphi)^2};$$

$$\psi_\varphi = \arccos \left(\frac{E_{int}^\varphi \cos \psi}{E_\varphi} \right) = \arcsin \left(-\frac{E_{ring}^\varphi + E_{int}^\varphi \sin \psi}{E_\varphi} \right).$$

The ellipticity coefficient can be calculated using the following formula:

$$K_e = \pm \sqrt{\frac{m \sin^2 \gamma - \sin 2\gamma \cos \psi_0 + (1/m) \cos^2 \gamma}{m \cos^2 \gamma + \sin 2\gamma \cos \psi_0 + (1/m) \sin^2 \gamma}},$$

where $m = E_\theta / E_\varphi$; $\psi_0 = \psi_\theta - \psi_\varphi$; $tg 2\gamma = \frac{2m \cos \psi_0}{m^2 - 1}$.

The polarization of the wave due to the interference radiation will not be circular in the direction of the polar axis ($\theta = 0$) as it can be inferred from expressions (27) and (28), where $E_\theta \neq E_\varphi$ and $E_\theta / E_\varphi \neq 1$. In case q has a significantly small value ($q \ll 1$), the ellipticity coefficient of the radiation along the annular antenna axis will be close to unity, satisfying the polarization requirements in communication lines. However, for metrological purposes, more stringent requirements for circular polarization quality should be met, and additional circuit or design solutions must be employed to reduce interference radiation.

4 EXPERIMENTS

The radiation in the direction of the ring axis of the ring antenna can serve as a standard reference for studying polarization characteristics of antennas. In such instances, the waves emitted by the power devices should be compensated. This can be achieved by designing the power supply circuit in such a way that its identical components form an anti-phase system of emitters. As a result, waves of equal intensity but opposite phases will be emitted in the direction of the ring axis, resulting in almost complete suppression of the interference intensity. Fig. 9 depicts the circuit diagram for supplying the ring antenna with two directional couplers placed symmetrically around the center of the circuit.

As shown in the diagram, all directional coupler elements are symmetrical in pairs concerning point O and are fed in an antiphase. The diagram indicates the phase shifts of the currents, and the arrows indicate the directions of the current wave propagation in the strip line segments.

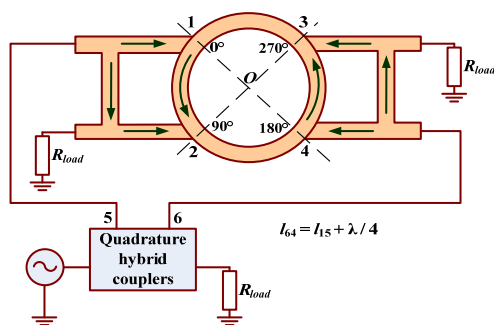


Figure 9 – The ring antenna with feeding by two branch-line directional couplers

The emission of interference radiation can also be mitigated through partial shielding of the power supply. Fig. 10 illustrates the ring antenna diagram with the opposite directional coupler's primary line placed behind the ring strip. In this configuration, the surface electromagnetic wave that may occur during the current wave propagation along the primary line will be contained within the dielectric layer between the two strips, there by considerably reducing unwanted radiation.

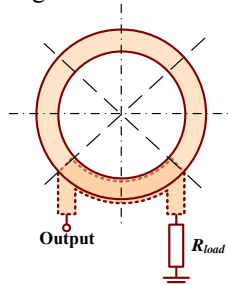


Figure 10 – The ring antenna in which the primary line of the directional coupler is located behind the ring strip

5 RESULTS

After analyzing the model shown in Fig. 9, the radiation pattern in two planes (as shown in Fig. 11) and the relationship between the wave ellipticity coefficient and frequency (as demonstrated in Fig. 12) were obtained. The VSWR did not exceed 1.4 within the operating frequency band. Moreover, the gain for the examined RHCP was not less than 6 dBi.

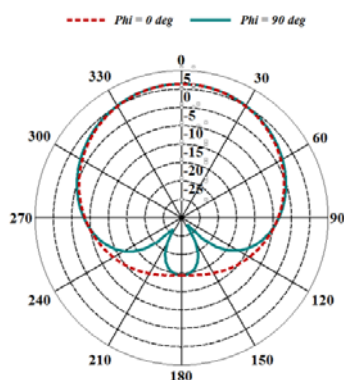


Figure 11 – The radiation patterns of ring antennas in two planes ($\varphi = 0$ and $\varphi = 90^\circ$) when supplied by two branch-line directional couplers

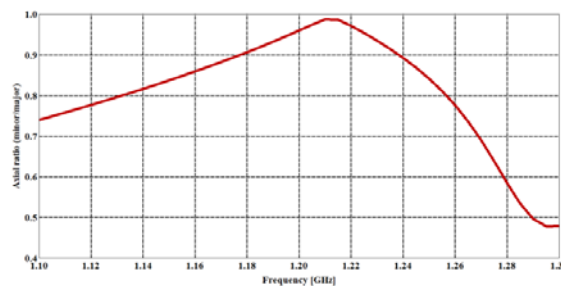


Figure 12 – Dependence of the ellipticity coefficient of ring antennas with supplying by two branch-line directional couplers on the operating frequency in the direction $\theta = 0$

The study results of the ring microstrip antenna with front electromagnetic coupling (as illustrated in Fig. 10) are presented in Fig. 13 and 14. The radiation pattern and the ellipticity coefficient as a function of frequency are shown in these figures, respectively. The VSWR value within the operating frequency range was not more than 1.1, and the gain for the investigated RHCP was at least 4 dBi.

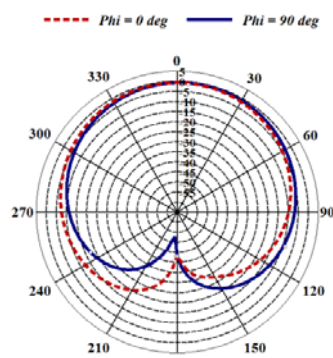


Figure 13 – The radiation patterns of ring antennas, in which the primary line of the directional coupler is located behind the ring strip, in two planes ($\varphi = 0$ and $\varphi = 90^\circ$)

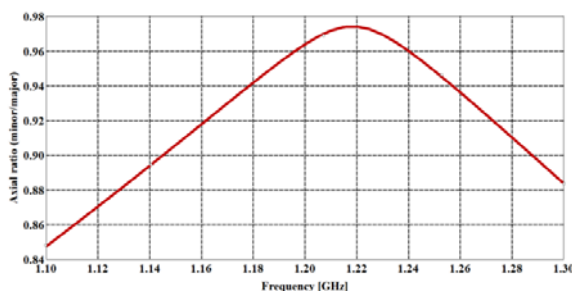


Figure 14 – Dependence of the ellipticity coefficient of ring antennas, in which the primary line of the directional coupler is located behind the ring strip, on the operating frequency in the direction $\theta = 0$

6 DISCUSSION

An analysis of the dependence graphs of the main characteristics of antennas with complex power supply circuits for directional couplers (Figs. 9 and Fig. 10) compared to similar characteristics for simple circuits (Fig. 1 and Fig. 2) showed that the radiation pattern shape in the upper radiation hemisphere became symmetric, especially when using a symmetrical supply of the ring

with branch-line couplers. Furthermore, the acceptable level of the ellipticity coefficient deviation at -3 dB has been maintained over a broader frequency range.

The branch-line directional coupler has another advantage over the coupler with electromagnetic coupling. This is the supply of the ring emitter with the full power of the power source with an efficiency close to unity. However, unlike the coupler with electromagnetic coupling, the branch-line coupler is more complex to calculate and design, and also occupies a large area on the printed circuit board. Therefore, it is sometimes advisable to use a ring antenna power supply circuit with two directional couplers with electromagnetic coupling, which are located symmetrically with respect to the ring axis.

CONCLUSIONS

The outcomes of the microstrip ring antenna modeling with power supply devices on directional couplers confirm the feasibility of constructing circularly polarized electromagnetic wave emitters that satisfy current technical standards.

The paper discusses factors that can have a detrimental effect on the frequency characteristics of ring antennas and the polarization purity of electromagnetic waves. The study also focuses on the mode of current wave propagation in supply lines. It was found that directional couplers with electromagnetic coupling can be utilized in the construction of receiving ring antennas, which prioritize efficiency over other parameters. Additionally, these antennas can be useful for polarization analysis of radiation fields.

The branch-line directional couplers, by dividing the output powers equally, enable the ring to be supplied with the maximum power from the high-frequency current generator, resulting in a highly efficient power supply for the ring.

The scientific novelty. The study has revealed that using a single-directional coupler in power circuits does not guarantee axial symmetry of the radiation field in the front half-space. The paper elucidates the underlying factors causing this phenomenon. It is demonstrated that symmetrical power supplies and shielding can overcome this issue and enhance the operating frequency range, as determined by the radiation field ellipticity coefficient.

The practical significance. After modelling prototypes of microstrip ring antennas, the results showed that the microstrip power line matched well with the radiating ring. The VSWR did not exceed 1.4 in the operating frequency band in all cases, and the gain for the type of polarization studied (RHCP) was not less than 4 dBi. The cross-polarization component's radiation was not higher than 15 dBi for sophisticated power supply circuits. The radiation pattern in the forward half-space became symmetrical concerning the antenna axis, especially with a symmetrical power supply.

Prospects for further research. Future research will focus on mathematical modeling and experimental study

of the utilization of symmetrical branch-line coupler circuits to power ring microstrip antennas for constructing antenna arrays.

REFERENCES

1. Ilnitsky L., Shcherbyna O., Yanovsky F., Zaliskyi M., Holubnychiy O., Ivanets O. Comparison of Circular and Linear Orthogonal Polarization Bases in Electromagnetic Field Parameters Measurement, *International Journal of Image, Graphics and Signal Processing*, 2022, Vol. 14, No. 3, pp. 58–72. DOI: 10.5815/ijigsp.2022.03.06
2. Ilnitsky L. Ya., Savchenko O. Y., Sibruk L. V. Anteny ta prystroji nadvysokykh chastot: pidruchnyk. Kyiv, Ukrtelecom, 2003, 496 p.
3. Li J., He B., Li L., Zhang A., Liu J., Liu Q. H. Capacitor-loaded circularly polarized annular-ring slotted microstrip patch antenna, *IEEE 11th International Symposium on Antennas, Propagation and EM Theory (ISAPE), China, 18–21 October, 2016: proceedings*. Guilin, 2016, pp. 13–15. DOI: 10.1109/ISAPE.2016.7833897
4. Huang J., Gong X. A Wide-Band Dual-Polarized Frequency Reconfigurable Slot-Ring Antenna Element Using a Diagonal Feeding Method for Array Design, *IEEE International Symposium on Antennas and Propagation and USNC/URSI National Radio Science Meeting, USA, 08–13 July, 2018: proceedings*. Boston, 2018, pp. 477–478. DOI: 10.1109/APUSNCURSINRSM.2018.8608781
5. Huang J., Gong X. A Tri-Band Dual-Polarized Slot-Ring Antenna for Array Design, *IEEE International Symposium on Antennas and Propagation and USNC/URSI National Radio Science Meeting, USA, 07–12 July, 2019: proceedings*. Atlanta, 2019, pp. 1151–1152. DOI: 10.1109/APUSNCURSINRSM.2019.8889188
6. Shirazi M., Huang J., Li T., Gong X. A Switchable-Frequency Slot-Ring Antenna Element for Designing a Reconfigurable Array, *IEEE Antennas and Wireless Propagation Letters*, 2018, Vol. 17, No. 2, pp. 229–233. DOI: 10.1109/LAWP.2017.2781463
7. Chen C., Li C., Zhu Z., Wu W. Wideband and Low Cross-Polarization Planar Annual Ring Slot Antenna, *IEEE Antennas and Wireless Propagation Letters*, 2017, Vol. 16, pp. 3009–3013. DOI: 10.1109/LAWP.2017.2757963
8. Godaymi Al-Tumah W. A., Shaaban R. M., Duffy A. P. Design, simulation, and fabrication of a double annular ring microstrip antenna based on gaps with multiband feature, *Engineering Science and Technology, an International Journal*, 2022, Vol. 29, pp. 1–10. DOI: 10.1016/j.jestch.2021.06.013
9. Phonkitiphan P., Kaewon R., Pancharoen K., Silapan P., Watcharakitchakorn O. Design of Graphene-Based Annular Ring Microstrip Antenna Using Short-Pin Technique for Dual Band Applications, *International Journal of Electrical and Electronic Engineering & Telecommunications*, 2020, Vol. 9, No. 4, pp. 231–236. DOI: 10.18178/ijeetc.9.4.231-236
10. Shcherbyna O., Ilnitsky L., Mykhalchuk I., Kozhokhina O. The Antenna Array with Ring Elements, *Signal Processing Symposium (SPSymposium 2017), Poland, 12–14 September, 2017: proceedings*. Jachranka, 2017, pp. 1–4. DOI: 10.1109/SPS.2017.8053700
11. Pozar M. D. *Microwave Engineering*: 4th edition. New Jersey, John Wiley & Sons, 2012. 756 p.
12. Gustrau F. *RF and Microwave Engineering: Fundamentals of Wireless Communications*. New Jersey, John Wiley & Sons, 2012. 368 p.

Received 10.04.2003.
Accepted 22.06.2023.

ЖИВЛЕННЯ КІЛЬЦЕВОЇ АНТЕНИ ЗА ДОПОМОГОЮ СПРЯМОВАНИХ ВІДГАЛУЖУВАЧІВ

Ільницький Л. Я. – д-р техн. наук, заслужений діяч науки і техніки України, Національний авіаційний університет, Київ, Україна.

Щербина О. А. – д-р техн. наук, професор кафедри електроніки, робототехніки і технологій моніторингу та інтернету речей, Національний авіаційний університет, Київ, Україна.

Заліський М. Ю. – д-р техн. наук, професор кафедри телекомунікаційних та радіоелектронних систем, Національний авіаційний університет, Київ, Україна.

Mykhalchuk I. I. – канд. техн. наук, асистент кафедри кібербезпеки та захисту інформації, Київський національний університет ім. Тараса Шевченка, Київ, Україна.

Кожохіна О. В. – канд. техн. наук, доцент кафедри авіоніки, Національний авіаційний університет, Київ, Україна.

АНОТАЦІЯ

Актуальність. В різних радіоелектронних системах застосовують радіохвилі з коловою поляризацією. Наприклад, це станції космічного зв'язку, деякі системи радіорелейного зв'язку, радіолокаційні станції, системи передачі даних і т.д. Електромагнітні хвилі, розкладені в коловому ортогональному поляризаційному базисі, використовують у системах радіомоніторингу та радіоконтролю, при дослідженнях особливостей поширення радіохвиль. Серед антен, які створені для приймання і випромінювання електромагнітних хвиль з коловою або обертовою поляризацією, за простотою конструкції та за електродинамічними характеристиками вигідно відрізняється кільцева антена.

Мета роботи – дослідження особливостей побудови та використання мікросмушкових спрямованих відгалужувачів для живлення кільцевих антен.

Метод. Для удосконалення пристроїв живлення мікросмушкових кільцевих антен та покращення їх властивостей розглядаються основні фактори, які викликають збуження робочого діапазону частот антени: частотна залежність параметрів спрямованого відгалужувача, коректність розрахунку схеми спрямованого відгалужувача, випромінювання несиметричних смужкових ліній. Обґрунтування впливу елементів живлення на характеристики кільцевої антени використовується зв'язок між полем випромінювання, аналітично визначене у власній системі координат, і полем випромінювання антени в основній системі координат.

Результати. Аналіз графіків залежностей основних характеристик кільцевих мікросмушкових антен з ускладненими схемами живлення спрямованих відгалужувачів і порівняння з аналогічними характеристиками для простих схем показало, що форма діаграми спрямованості у верхній півсфері випромінювання стала симетричною відносно осі, особливо у випадку симетричного живлення кільця шлейфовими відгалужувачами. Також розширився діапазон частот, у якому відхилення коефіцієнту еліптичності від одиниці знаходиться на допустимому рівні.

Висновки. Результати моделювання мікросмушкових кільцевих антен з лініями живлення на спрямованих відгалужувачах різних типів показали, що збудження кільця за допомогою спрямованого відгалужувача забезпечує випромінювання електромагнітних хвиль коловою поляризацією. При цьому діапазон робочих частот, у якому залишається на допустимому рівні -3дБ відхилення коефіцієнту еліптичності досить широкий. Живлення кільцевої антени пристроями, побудованими на шлейфових спрямованих відгалужувачах, дає можливість за допомогою однієї кільцевої антени одночасного випромінювання хвиль з правим та лівим напрямом обертання вектора напруженості електричного поля.

КЛЮЧОВІ СЛОВА: мікросмушкова кільцева антена, спрямований мікросмушковий відгалужувач, лінії живлення, коефіцієнт еліптичності, основна система координат, власна система координат.

ЛІТЕРАТУРА

1. Comparison of Circular and Linear Orthogonal Polarization Bases in Electromagnetic Field Parameters Measurement / [L. Ilitsky, O. Shcherbyna, F. Yanovsky et al.] // International Journal of Image, Graphics and Signal Processing. – 2022. – Vol. 14, No. 3. – P. 58–72. DOI: 10.5815/ijigsp.2022.03.06
2. Ільницький Л. Я. Антени та пристрої надвисоких частот: підручник для ВНЗ / Л. Я. Ільницький, О. Я. Савченко, Л. В. Сібрук. – К.: Укртелеком, 2003. – 496 с.
3. Capacitor-loaded circularly polarized annular-ring slotted microstrip patch antenna / [J. Li, B. He, L. Li et al.] // IEEE 11th International Symposium on Antennas, Propagation and EM Theory (ISAPE), China, 18–21 October, 2016: proceedings. – Guilin, 2016. – P. 13–15. DOI: 10.1109/ISAPE.2016.7833897.
4. Huang J. A Wide-Band Dual-Polarized Frequency Reconfigurable Slot-Ring Antenna Element Using a Diagonal Feeding Method for Array Design / J. Huang, X. Gong // IEEE International Symposium on Antennas and Propagation and USNC/URSI National Radio Science Meeting, USA, 08–13 July, 2018: proceedings. – Boston, 2018. – P. 477–478. DOI: 10.1109/APUSNCURSINRSM.2018.8608781.
5. Huang J. A Tri-Band Dual-Polarized Slot-Ring Antenna for Array Design / J. Huang, X. Gong // IEEE International Symposium on Antennas and Propagation and USNC/URSI National Radio Science Meeting, USA, 07–12 July, 2019: proceedings. – Atlanta, 2019. – P. 1151–1152. DOI: 10.1109/APUSNCURSINRSM.2019.8889188
6. A Switchable-Frequency Slot-Ring Antenna Element for Designing a Reconfigurable Array / [M. Shirazi, J. Huang, T. Li, X. Gong] // IEEE Antennas and Wireless Propagation Letters. – 2018. – Vol. 17, No. 2. – P. 229–233. DOI: 10.1109/LAWP.2017.2781463
7. Wideband and Low Cross-Polarization Planar Annual Ring Slot Antenna / [C. Chen, C. Li, Z. Zhu, W. Wu] // IEEE Antennas and Wireless Propagation Letters. – 2017, Vol. 16. – P. 3009–3013. DOI: 10.1109/LAWP.2017.2757963
8. Godaymi Al-Tumah W. A. Design, simulation, and fabrication of a double annular ring microstrip antenna based on gaps with multiband feature / W. A. Godaymi Al-Tumah, R. M. Shaaban, A. P. Duffy // Engineering Science and Technology, an International Journal. – 2022. – Vol. 29. – P. 1–10. DOI: 10.1016/j.jestch.2021.06.013
9. Design of Graphene-Based Annular Ring Microstrip Antenna Using Short-Pin Technique for Dual Band Applications / [P. Phonkitiphan, R. Kaewon, K. Pancharoen et al.] // International Journal of Electrical and Electronic Engineering & Telecommunications. – 2020. – Vol. 9, No. 4. – P. 231–236. DOI: 10.18178/ijeetc.9.4.231-236
10. The Antenna Array with Ring Elements / [O. Shcherbyna, L. Ilitsky, I. Mykhalchuk, O. Kozhokhina] // Signal Processing Symposium (SPSymo 2017), Poland, 12–14 September, 2017: proceedings. – Jachranka, 2019. – P. 1–4. DOI: 10.1109/SPS.2017.8053700
11. Pozar M. David. Microwave Engineering: 4th edition / M. David Pozar. – New Jersey: John Wiley & Sons, 2012. – 756 p.
12. Gustrau F. RF and Microwave Engineering: Fundamentals of Wireless Communications / F. Gustrau. – New Jersey: John Wiley & Sons, 2012. – 368 p.